# **Research Article**

# Therapeutic efficacy of an oncolytic adenovirus containing RGD ligand in minor capsid protein IX and Fiber, $\Delta 24$ DoubleRGD, in an ovarian cancer model

Lena J. Gamble<sup>1,6</sup>, Hideyo Ugai<sup>1,6</sup>, Minghui Wang<sup>1,6</sup>, Anton V. Borovjagin<sup>2,6</sup> and Qiana L. Matthews<sup>1,3,4,5,6</sup>

<sup>1</sup>Division of Human Gene Therapy, Departments of Medicine, Pathology, Surgery, Obstetrics and Gynecology; <sup>2</sup>School of Dentistry, Institute of Oral Health Research; <sup>3</sup>the Gene Therapy Center; <sup>4</sup>Center for AIDS Research; <sup>5</sup>Division of Infectious Diseases; <sup>6</sup>University of Alabama at Birmingham, Birmingham, Alabama 35294, USA

Received on October 26, 2011; Accepted on December 27, 2011; Published on February 15, 2012

Correspondence should be addressed to Qiana L. Matthews; Phone: +1 205 934-0573, Fax: +1 205 934-5600, E-mail: qlm@uab.edu

#### **Abstract**

Ovarian cancer is the leading cause of gynecological disease death despite advances in medicine. Therefore, novel strategies are required for ovarian cancer therapy. Conditionally replicative adenoviruses (CRAds), genetically modified as anti-cancer therapeutics, are one of the most attractive candidate agents for cancer therapy. However, a paucity of coxsackie B virus and adenovirus receptor (CAR) expression on the surface of ovarian cancer cells has impeded treatment of ovarian cancer using this approach.

This study sought to engineer a CRAd with enhanced oncolytic ability in ovarian cancer cells, " $\Delta 24$ DoubleRGD."  $\Delta 24$ DoubleRGD carries an arginine-glycine-aspartate (RGD) motif incorporated into

both fiber and capsid protein IX (pIX) and its oncolytic efficacy was evaluated in ovarian cancer. *In vitro* analysis of cell viability showed that infection of ovarian cancer cells with  $\Delta 24$ DoubleRGD leads to increased cell killing relative to the control CRAds. Data from this study suggested that not only an increase in number of RGD motifs on the CRAd capsid, but also a change in the repertoir of targeted integrins could lead to enhanced oncolytic potency of  $\Delta 24$ DoubleRGD in ovarian cancer cells *in vitro*. In an intraperitoneal model of ovarian cancer, mice injected with  $\Delta 24$ DoubleRGD showed, however, a similar survival rate as mice treated with control CRAds.

## Introduction

Ovarian cancer is the leading cause of gynecologic disease death (Jemal et al. 2008). In 2009 there were approximately 21,990 new cases of ovarian cancer and 15,460 deaths from this disease in the United States alone (NCI 2009). Traditional treatments have improved over the past several decades, but the 5-year survival rate of women diagnosed with ovarian cancer remains below 50% (Choi et al. 2008). To improve the outcomes achieved using ovarian cancer therapy, novel treatment regimen and modalities have been proposed in the past several years. One such novel treatment involves the use of conditionally replicative adenoviruses (CRAds) as cancer therapeutic agents (Barnes et al. 2002). Several considerations must be taken into account for effective use of CRAds: 1) selective infection of cancer cells versus non-cancer cells, 2) specific

killing of cancer cells versus normal cells, and 3) in vivo stability of the virus.

Wild type adenovirus (Ad) infections cause a natural cytolytic effect on target cells, resulting from viral replication that leads to cell destruction. Newly released progeny particles then laterally spread to and infect adjacent target cells in repetitive cycles, leading to gradual destruction of infected tissue (Kirn 2000). CRAds, oncolytic Ads, can be generated through manipulation of the Ad genome. These manipulations allow preferential replication of the virus in cancer cells, and as a result, Ad viruses selectively kill cancer cells via their naturally lytic replication cycle (Heise et al. 2000, Heise & Kirn 2000). The utility of CRAds has been underscored by their rapid transition to clinical trials. One type of CRAd was developed by means of deleting 24 base pairs (bps) from the immediate early E1A gene of the viral genome (Fueyo et al.

© The Author(s) 2012. Published by Lorem Ipsum Press.

2000). This CRAd, known as "delta-24" ( $\Delta$ 24), fails to replicate in non-cancer cells because the deletion disrupts the ability of EIA to bind to tumor suppressor retinoblastoma protein, Rb (Fueyo et al. 1996). This function of E1A is critical for initiation of Ad DNA replication in normal cells, because the binding of E1A to Rb is required to overcome the G1-S checkpoint (Nevins 1992, Whyte et al. 1988, 1989). However, the 24-bp deficiency is overcome in many cancer types (Sherr 1996), including ovarian cancer (Liu et al. 1994, Yaginuma et al. 1997, Niederacher et al. 1999), due to disruption of the p16/Rb pathway. As a consequence,  $\Delta 24$ CRAd replication occurs in a cancerselective manner in ovarian cancer cells.

Ovarian cancer cells have been found to express variable and often reduced levels of coxsackie B virus and adenovirus receptor (CAR), the primary receptor for Ad serotype 5 (Ad5), resulting in inefficient adenovirus transduction (Kelly et al. 2000, Vanderkwaak et al. 1999, Khuu et al. 1999). However, α<sub>ν</sub>β integrins, have been shown to be expressed in abundance on ovarian cancer cells (Liapis et al. 1997, Cannistra et al. 1995). Therefore, tropism modification strategies have been employed to increase infectivity of ovarian cancer cells. In particular, insertion of a ligand with an arginine-glycine-aspartate (RGD) motif in the HI loop of the fiber knob domain allows the Ad vector to effectively target ovarian cancer cells through the RGD motif (Dmitriev et al. 1998, Bauerschmitz et al. 2002). One advantage of RGD-modified Ad vectors is that they have been determined to be more resistant to Ad5 -neutralizing antibodies in vivo than the unmodified vector (Wang et al. 2005). Moreover, a CRAd containing a fiber-incorporated RGD motif, Ad5-Δ24RGD, demonstrates increased infectivity in ovarian cancer cells (Suzuki et al. 2001), resulting in effective killing of those cells (Whyte et al. 1989). Furthermore, Ad5-Δ24RGD shows an excellent safety profile in cotton rats (Page et al. 2007) and was recently evaluated in a Phase I trial for patients with recurrent ovarian cancer (Kimball et al. 2010). Thus, RGD-mediated transduction of Ad appears to be effective for targeting ovarian cancer. Based on these observations, we reasoned that further modification of Ad5-Δ24RGD (herein referred to as Δ24FiberRGD) could improve oncolytic potency and possibly therapeutic efficacy by augmenting its ability to bind to integrins on ovarian cancer cells.

Protein IX biochemical and structural localization studies have demonstrated that the C-terminus of this protein can efficiently present ligands genetically fused to it without detrimentally affecting the capsid assembly and the viral infectivity. Ability of ligand-modified pIX to mediate Ad transduction has also been reported (Dmitriev et al. 1998, Meulenbroek et al. 2004, Vellinga et al. 2004, Dmitriev et al. 2002, Campos et al. 2004). Based on these data, we hypothesized that simultaneous incorporation of the RGD motif in pIX and Fiber would enhance Ad infectivity and cell killing activity. Therefore, we genetically modified the Cterminus of the pIX gene of  $\Delta 24$ RGD with the nucleotide sequence for an RGD motif to generate Δ24DoubleRGD which contains the RGD motif in both pIX and Fiber, yielding a virus expressing up to 276 (240 pIXs + 36 fibers) copies of the RGD-ligand. We examined the biological and physical properties of Δ24DoubleRGD and evaluated its oncolytic ability in vitro and in vivo. Due to its ability to induce oncolysis of ovarian cancer cells in vitro and in vivo to an extent similar to or greater than  $\Delta 24$ FiberRGD, we believe the Δ24DoubleRGD may be useful as a potential ovarian cancer therapeutic.

#### **Materials and Methods**

#### Cells

Human embryonic kidney 293 (HEK293) cells (CRL 1573) and human lung epithelial A549 cells (ATCC CCL 185) were purchased from American type culture collection (ATCC, Manassas, VA). HEK293 cells and A549 cells were used for production and amplification of viruses, respectively. SKOV3.Luc cells were a kind gift from Dr. Robert Negrin (Stanford Medical School, Stanford, CA). The human ovarian cancer cell line, SKOV3.Luc, which stably expresses luciferase, was used for in vitro and in vivo experiments. Cells were maintained in DMEM/F-12 (Sigma-Aldrich; St. Louis, MO) supplemented with the following: 10% Fetal Bovine Serum (FBS; Invitrogen Carlsbad, CA), 2 mM Lglutamine (Sigma), 100 IU/ml penicillin (Sigma) and 100 μg/ml streptomycin (Sigma). Cells were incubated in humidified atmosphere in 5% CO<sub>2</sub> at 37°C. The adenovirus-infected cells were cultured in the same medium containing 2% FBS.

## Recombinant plasmids

To construct the pShuttle plasmid needed to create the p Δ 2 4 I X F l a g 4 5 Å R G D pΔ24IXFlag45ÅRGDFiberRGD genomes (rescue vecwe replaced the tk portion of the pSlΔ24pIXNheFlag-tk (Kimball et al. 2009), with 45ÅRGD, which was PCR-amplified from previously constructed pSl\Delta E1/CMV-luc, 45\Delta RGD shuttle plasmid (Borovjagin et al., unpublished data). The pSlΔ24IXFlag45ÅRGD shuttle vector and pTG3602 backbone (Chartier et al. 1996) were digested with PmeI and ClaI, respectively, and were subjected to homologous recombination in Escherichia coli (E. coli) strain BJ5183 (Stratagene, La Jolla, CA).

The resulting vector, pΔ24IXFlag45ÅRGD, was used to generate Δ24IXRGD virus with wt fiber as a control.

To construct pΔ24IXFlag45ÅRGDFiberRGD, pSl\D24IXFlag45\hat{A}RGD shuttle vector was recombined with the pVK503C backbone plasmid (Dmitriev et al. 1998), which contains a modified (DAM methylationproof) ClaI site in the E1 region and the RGD4C modification in the fiber knob HI-loop sequence. The shuttle vector and backbone plasmid were digested with PmeI and ClaI, respectively, and were homologously recombined in BJ5183. The resulting plasmid, pΔ24IXFlag45ÅRGDFiberRGD was used to generate Δ24DoubleRGD. This sequence has been deposited into GenBank and the accession number is JF745946.

#### Adenoviruses

Plasmids pSlΔ24IXFlag-45ÅRGD and pSlΔ24IXFlag-45ÅRGDFiberRGD, were digested with PacI, and transfected into HEK293 cells in a 25cm<sup>2</sup> flask using Lipofectamine 2000<sup>TM</sup> (Invitrogen) in order to generate Δ24IXRGD and Δ24DoubleRGD, respectively. The transfected cells were incubated for approximately two weeks until full cytopathic effect (CPE) was induced by the recombinant CRAds. After observation of CPE, we collected infected cells with medium and harvested by centrifugation at 3,000 × g for 5 minutes (min) at 4°C. The cell pellet was resuspended in 5 ml of medium, and disrupted using four freeze and thaw cycles to release virus into the medium. Cell debris was removed by centrifugation at 3,000 × g for 5 min at 4°C, and the supernatant was used to scale up adenoviruses.

We also used two other CRAds, Δ24Ad5 ( $\Delta 24$ ) (Fueyo et al. 2000), and Ad5- $\Delta 24$ RGD (Δ24FiberRGD) (Suzuki et al. 2001) to compare with  $\Delta$ 24DoubleRGD in this study. The  $\Delta$ 24Ad5 was kindly provided by Dr. Juan Fueyo (The University of Texas, Center, Anderson Houston, M.D. TX). Δ24FiberRGD was manufactured under Good Laboratory Practice (GLP) conditions at the Biopharmaceutical Development Program (SAIC-Frederick, Frederick, MD) with support from the National Cancer Institute Rapid Access to Intervention Development program.

#### Purification and titration of adenoviruses

Each of the CRAds were amplified at the University of Alabama at Birmingham according to previously established protocols. Briefly, CRAds were propagated in A549 cells up to 15 flasks of 175 cm<sup>2</sup> and purified by double CsCl density gradient centrifugation followed by dialysis against phosphate-buffered saline (PBS [pH 7.4]) containing 10% glycerol for purification (Maizel et al. 1968). The infectious titer (PFU/ml)

of each virus was determined by titration in 293 cells as previously described (Borovjagin et al. 2010). The particle titer (vp/ml) was determined by A<sub>260</sub> absorbance of purified particles and assuming that  $1.1 \times 10^{12}$ vp/ml has an absorbance of 1.0 at 260 nm, as previously described (Maizel et al. 1968). All viruses were stored at -80°C until use.

## Sequencing

All viruses were verified by sequencing provided by the Center for AIDS Research (CFAR) and Comprehensive Cancer Center (CCC) DNA Sequencing and Analysis Core at the University of Alabama at Birmingham according to previously established protocols.

# Western Blot Analysis

Samples containing  $5.0 \times 10^9$  vp of purified virus were boiled in Laemmli sample buffer for 5 minutes and analyzed by a 4 to 15% gradient sodium dodecyl sulfate-polyacrylamide gel electrophoresis (SDS-PAGE). Separated proteins were transferred to polyvinylidene difluoride (PVDF) membrane. PVDF membrane was blocked in 5% skim milk in Tris-buffered saline (pH 7.5) containing 0.05% Tween 20 (TBST) followed by incubation with primary antibodies (mouse monoclonal anti-flag M2 primary antibody (Sigma) or mouse monoclonal anti-Fiber antibody [4D2] 1:5000 (Thermo Scientific, Rockford, IL). The membranes were washed with TBST, blocked with TBST containing 5% skim milk, and incubated with the appropriate secondary goat anti-mouse antibodies conjugated with horse radish peroxidase (HRP) at 1:1000 dilution. The HRP signal was developed with ECL plus Western blotting detection system (GE healthcare, Little Chalfont, UK) then detected with BioMax MR scientific imaging films (Kodak, Chalon-sur-Saone, France) using a medical film processor SRX-101A (Konica, Tokyo, Japan). Pre-stained protein ladder of Kaleidoscope Standard (Bio-Rad Laboratories, Inc.) was used to estimate protein sample sizes.

## Enzyme-linked Immunosorbent Assay (ELISA) $\alpha_{\nu}\beta_{3}$ or $\alpha_{\nu}\beta_{5}$ ELISA

Purified  $\alpha_v \beta_3$  or  $\alpha_v \beta_5$  integrins (Millipore, Billerica, MA) were diluted in 50 mM bicarbonate buffer (pH 9.5) to a final concentration of 1 µg/ml, and 200 µl aliquots were added to each well of a 96-well Nunc-Maxisorp ELISA plate (Nunc Maxisorp, Rochester, NY). Plates were incubated for 2 hours at room temperature to bind purified  $\alpha_v \beta_3$  or  $\alpha_v \beta_5$  integrins on the wells then washed four times with 200 µl of wash buffer (PBS containing 0.1% Tween 20; PBST). Samples were blocked for 1 hour at room temperature by the addition of 100 µl blocking buffer (washing buffer containing 3% bovine serum albmin). The plate was incubated for 2 hours at room temperature to allow CRAds to bind to integrins. The wells were washed three times with 200 µl PBST then blocked with 100 µl blocking buffer for 1 hour at room temperature. Next we added anti-Ad5 sera (recovered from mice exposed to Ad) as a primary antibody to each well at a ratio of 1:100 in 100 µl blocking buffer, and incubated the plate for 2 hours at room temperature. The wells were washed three times with 200 µl of PBST then blocked with 100 µl blocking buffer for 1 hour at room temperature. Polyclonal goat anti-mouse antibody conjugated with HRP (Dako, Denmark, A/S) at 1:2000 dilution in blocking buffer was added for 2 hours at room temperature, followed by addition of 100 µl of SigmaFast OPD solution in 20 ml of deionized water (Sigma). Plates were incubated for 1 hour at room temperature, and colorimetric changes were read at OD<sub>405</sub> nm using a 96-well plate reader (PowerWave HT340, Biotek). Each virus-integrin interaction was repeated in three wells and results are displayed as one point on a graph with bars indicating standard error.

#### Flag ELISA

Viruses were added to a Nunc-Maxisorp ELISA plate at the indicated concentrations. The plate was incubated for 2 hours at room temperature to allow CRAds to bind to plate. The wells were washed three times with 200 µl PBST then blocked with 100 µl blocking buffer for 1 hour at room temperature. Next we added anti-Flag antibody conjugated to HRP at a ratio of 1:1000 in blocking buffer and incubated at room temperature for 2 hours. The wells were washed three times with 200 µl of PBST then 100 µl of SigmaFast OPD solution was added to each well. Plates were incubated for 1 hour at room temperature, and colorimetric changes were read at OD<sub>405</sub> nm using a 96-well plate reader (PowerWave HT340, Biotek). Each virusintegrin interaction was repeated in three wells and results are displayed as one point on a graph with bars indicating standard error.

## Analysis of cell viability by MTS Assay

SKOV3.Luc cells were plated in a 96-well plate at 1 × 10<sup>4</sup> cells per well and grown overnight. The following day, CRAds were diluted with medium containing 2% FBS, and cells were infected with Multiplicities of Infection (MOIs) of 0 (no virus), 0.1, 1.0, 10, 50, 100, or 1,000 vp/cell. Infected cells were incubated for 10 days. MTS assay was performed using the CellTiter 96 AQueous One Solution Cell Proliferation Assay (Promega, Madison, WI) according to the manufacturer's instructions. Colorimetric differences were

measured at OD<sub>490</sub> nm using a 96-well plate reader. Each MOI was repeated in three wells and data are displayed as one point on the graph with bars indicating standard error. Each experiment was performed three times and only one graph is displayed as a representation of the data collected.

#### **Crystal Violet staining**

Crystal violet assay was used to determine the oncolytic effect of the CRAd agents on SKOV3.Luc cells following infection. We seeded  $1 \times 10^4$  cells per well in 96-well plates, and incubated cells overnight. Cells were infected with CRAds at MOIs of 0 (no virus), 0.1, 1.0, 10, 50, 100, or 1,000 vp/cell and incubated for 10 days at 37°C. On Day 10, medium was removed and infected cells were gently washed with PBS [pH 7.4) and incubated with Crystal Violet solution (1% Crystal Violet in 70% ethanol) for 1 hour. Cells were washed three times with water then allowed to air dry overnight. We captured images of Crystal Violet solution staining levels with a JVC Everio HD digital cam-

#### **Luciferase Assav**

We assessed cell viability using luciferase activity as a readout of remaining living cells following CPE induction by CRAds. We seeded  $1.0 \times 10^4$  SKOV3.Luc cells/well in a 96-well plate and incubated overnight. Cells were infected with CRAds at MOIs of 0 (no virus), 0.1, 1.0, 10, 50, 100, or 1000 vp/cell for 10 days. Ten days post-infection, medium was aspirated and infected cells were gently washed with PBS (pH 7.4). Infected cells were lysed with 50 µl of passive lysis buffer (Promega, Madison, WI) for 15 minutes at 37°C and the lysates were transferred to 1.5-ml tubes. Luciferase assay was performed according to the manufacturer's protocol and the relative light unit (RLU) readout was normalized to the amount of protein present as determined by Dc protein assay (BioRad, Hercules, CA). Each MOI was repeated in three wells and data are displayed as one point on the graph with bar indicating standard error. Each experiment was performed three times and only one graph is displayed as a representation of the data collected.

# Orthotopic ovarian cancer tumor model

The University of Alabama at Birmingham Institutional Animal Use and Care Committee approved the use of mice as described herein under the approved protocol number 090907606. Seventy-five BALB/c nude mice, divided into five groups with 15 mice per group, were used for the orthotopic ovarian cancer model. SKOV3.Luc cells were cultured using techniques described above then trypsinized and counted. Trypan blue exclusion was used to determine that cell viability was > 98%. Cells were washed two times with PBS. SKOV3.Luc cells  $(1\times10^7)$  in 1000 µl of PBS were injected intraperitoneally (IP) into mice 6 days prior to first injection with CRAd or PBS (Day -6). CRAd (1×10<sup>9</sup> vp) or PBS was injected IP in 1000 ul of PBS once per week for 3 weeks on Days 0, 7, and 14. Bioluminescent imaging of tumors was performed every 7 days. For imaging, 150 mg/kg luciferin (Xenogen Corporation, Alameda, CA) was injected IP into mice. After 10-20 minutes, mice were placed in the imaging chamber and maintained under anesthesia with 2% isoflurane gas (Minrane Inc., Bethleham, PA) at a flow rate of approximately 0.5-1.0 1/min per mouse (Highland Medical Equipment, Temecula, CA). Imaging was completed using a Xenogen IVIS 100 camera ( Xenogen Corporation, Alameda, CA). Data were analyzed using Living Image software edition 3.1 (Caliper Life Sciences, Hopkinton, MA).

#### **Statistical Analysis**

Statistical significance between groups was assessed using Student's t-test calculations formulated for a two -tailed analysis of two sets of data. A cutoff of P <0.05 was used to determine statistical significance.

#### Results

# Confirmation of the integrity and viability of **∆24DoubleRGD**

Δ24DoubleRGD was generated as described in the Materials and Methods section. Direct sequencing of the purified CRAd genomes confirmed the nucleotide sequences of the RGD4C ligand inserted at both the fiber knob HI-loop and downstream of the pIX gene (data not shown). Figure 1 shows a schematic representation of the CRAds used in this study. We first verified composition of the viral structural proteins using purified viral particles by coomassie blue staining. The viral structural proteins (Hexon, Penton base, and the doublet pIIIa and Fiber) of  $\Delta$ 24DoubleRGD as well as those of the control viruses were similarly stained by coommassie blue (Figure 2A). Therefore, modifications of pIX and fiber using the RGD motif did not appear to affect composition of the viral structural proteins. Western blot analysis of purified viral particles using anti-pIX antibody showed the presence of wild type pIX in  $\Delta 24$ Ad5 and  $\Delta 24$ FiberRGD virus particles at 14 kDa, which is the expected molecular weight of unmodified pIX (Figure 2B). Virus particles of Δ24IXRGD and Δ24DoubleRGD show, however,

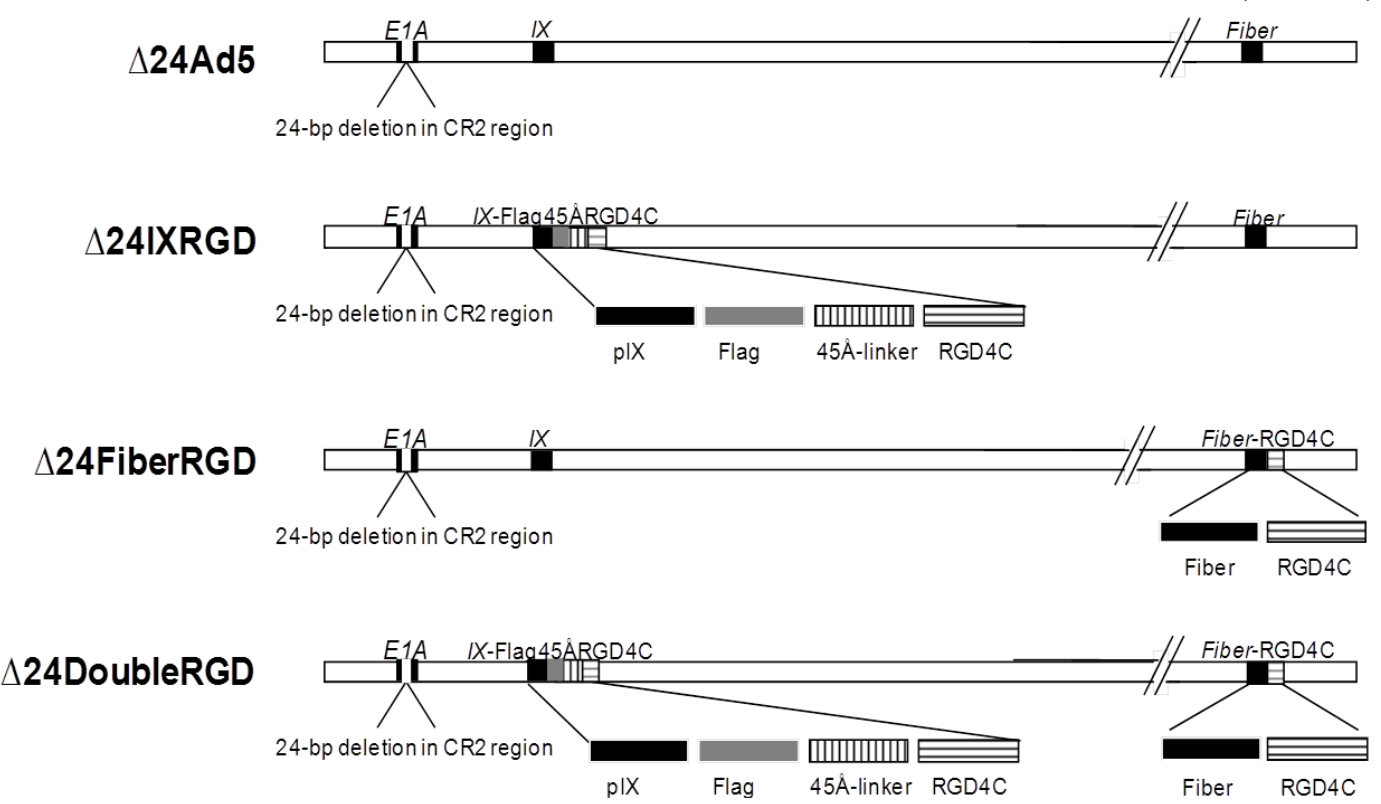


Figure 1. Each of the CRAds used for these experiments contained a 24-bp deletion in the pRb-binding region of the immediate early gene ( $\Delta 24$ ). The virus that contains only this modification is  $\Delta 24Ad5$ . The modification at the gene encoding protein IX contains a fusion cassette that includes: Flag protein, a 45Ålinker, and the RGD4C motif. This fusion modification was incorporated into the  $\Delta 24$ IXRGD. The Fiber modification incorporates the RGD4C motif in  $\Delta 24$ FiberRGD. The Δ24DoubleRGD was engineered to incorporate both the fusion modification at pIX and the RGD4C motif at Fiber.

bands that resolved at 21.8 kDa, which is the expected molecular weight of pIX and the fusion protein. A degradation product (or possibly a protein band that crossreacts with the primary or secondary antibody) pIX-RGD was detected in the  $\Delta 24$ DoubleRGD and Δ24RGD viral particles and marked with an asterisk (\*). Western blot analysis of pIX presence in CRAds indicates differential weight of pIX in viruses corresponding to fusion protein presence. Western blot analysis of purified viral particles using the Flagspecific monoclonal antibody confirmed that the 21.8 kDa band seen in the Δ24IXRGD and Δ24Double RGD samples contain the Flag epitope, a part of the fusion protein added to pIX (Figure 2C). In contrast, no protein was detected for Δ24Ad5 or Δ24FiberRGD due to lack of incorporation of the Flag-tag sequence into the pIX region of these CRAds.

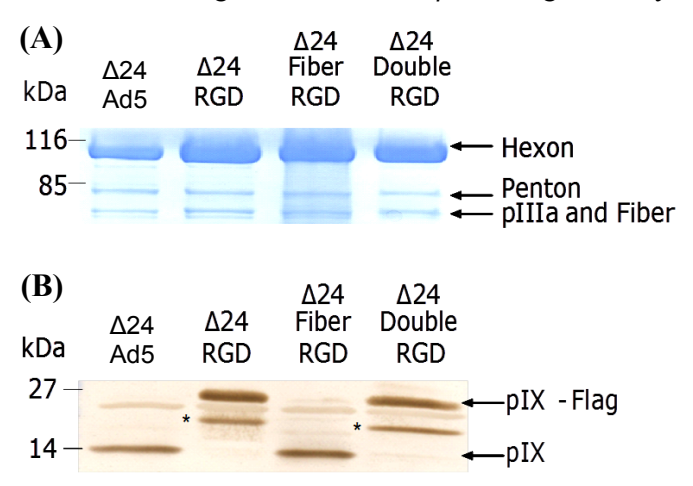
Next, we confirmed quantitatively that pIX on the viral particles was modified by a fusion peptide containing the Flag epitope by ELISA assay using anti -Flag antibody conjugated to HRP (Flag-HRP). ELISA analysis revealed Flag-HRP bound to Δ24IXRGD and Δ24DoubleRGD in a concentration-dependent manner, but not to  $\Delta 24Ad5$  and  $\Delta 24FiberRGD$  (Figure 2D). This suggests Δ24IXRGD and Δ24DoubleRGD viral particles displayed the modified pIX protein.

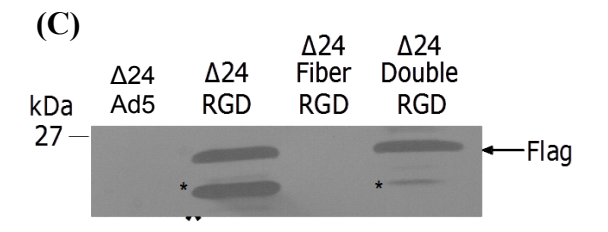
Taken together, these data confirm the incorporation of normal proteins into the capsids of the newly created CRAds. Furthermore, the presence of the fusion protein containing: Flag, 45Å, and RGD motifs in the pIX region, was identified in both Δ24IXRGD and Δ24DoubleRGD.

# $\Delta 24$ DoubleRGD is capable of binding to $\alpha_v \beta_3$ and α<sub>ν</sub>β<sub>5</sub> integrins

We next assessed whether  $\Delta 24IXRGD$  $\Delta 24$ DoubleRGD viral particles interacted with  $\alpha_{\rm v}\beta_3$ and  $\alpha_v \beta_5$  integrins by ELISA. Figure 3A showed that both Δ24IXRGD and Δ24DoubleRGD effectively bound  $\alpha_v \beta_3$  integrin in a dose-dependent manner. While Δ24Ad5 and Δ24FiberRGD had a lesser interaction with  $\alpha_v \beta_3$  integrin, both CRAds registered an interaction greater than 0. This is an expected result because each of the CRAds contain RGD in their penton base motifs which are known to interact with  $\alpha_v \beta_3$ .  $\Delta 24$ FiberRGD does bind  $\alpha_{v}\beta_{3}$  better than  $\Delta 24$ Ad5. The binding of  $\Delta 24$ FiberRGD to  $\alpha_v \beta_3$  is significantly greater than the binding of  $\Delta 24Ad5$  to  $\alpha_v\beta_3$  at concentrations greater than or equal to  $12.5 \times 10^8$  vp/ml. For concentrations equal to or lower than  $6.3 \times 10^8$  vp/ml there was no significant difference between the binding of  $\Delta 24$ Ad5 and  $\Delta 24$ FiberRGD to  $\alpha_v \beta_3$ ; however, there was significantly more binding of both  $\Delta 24$ pIXRGD and  $\Delta 24$ DoubleRGD to  $\alpha_v \beta_3$  than

 $\Delta 24$ Ad5 at these same concentrations (Figure 3A). Δ24DoubleRGD, Δ24IXRGD, and Δ24FiberRGD each similarly recognized  $\alpha_v \beta_5$  integrin in a dose-dependent manner (Figure 3B); the differences between binding of each of these CRAds to  $\alpha_v \beta_5$  was not statistically significant. Binding of  $\Delta 24Ad5$  to  $\alpha_v\beta_5$  was significantly





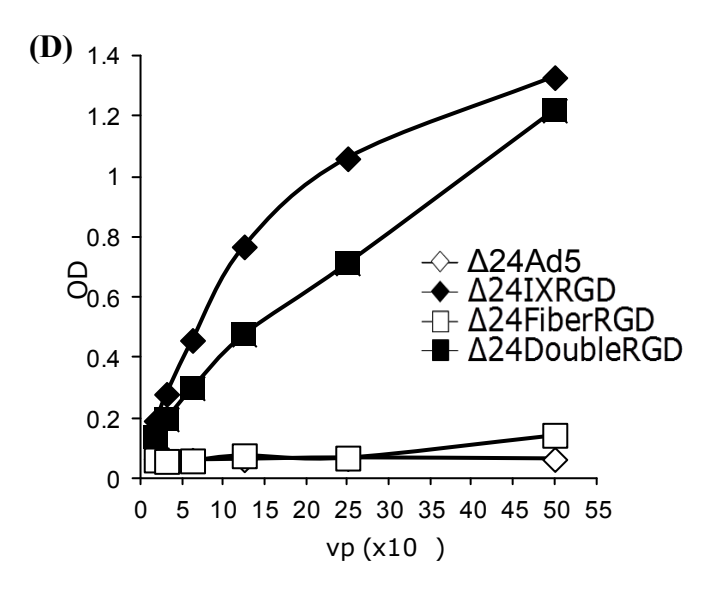


Figure 2. Coomassie stain verifies the presence of major Ad proteins: Hexon, Penton, and protein III and Fiber in each of the CRAds (A). pIX presence in each virus was verified by Western blot analysis (B). Flag incorporation into Δ24IXRGD and Δ24DoubleRGD was confirmed using Western blot analysis (C) and ELISA (D). Asterisks (\*) indicate degradation products of the fusion protein in (B) and (C).

lower than binding of Δ24IXRGD, Δ24FiberRGD, and  $\Delta 24$ DoubleRGD at or above  $6.3 \times 10^8$  vp/ml. The trend of greater binding of each of the CRAds to  $\alpha_v \beta_5$ versus  $\Delta 24Ad5$  binding to  $\alpha_v\beta_5$  continued throughout all of the concentrations. Notably, the binding of  $\Delta 24$ Ad5 to  $\alpha_v \beta_5$  was above zero due to the presence of RGD on penton base interacting with  $\alpha_v \beta_5$ .

# Cell killing activity of A24DoubleRGD is enhanced as compared to A24FiberRGD in vitro

To assess in vitro cell killing activity Δ24DoubleRGD in ovarian cells, we performed crystal violet analysis. Crystal violet analysis using SKOV3.Luc cells demonstrated that cell killing activity of Δ24DoubleRGD was increased as compared to  $\Delta$ 24Ad5,  $\Delta$ 24IXRGD, and  $\Delta$ 24FiberRGD (Figure 4A). We also quantified cell killing activity of Δ24DoubleRGD as compared with the other CRAds using MTS assay. Δ24DoubleRGD showed similar cell killing ability to  $\Delta 24Ad5$  and significantly better cell killing than  $\Delta 24IXRGD$  (p=0.0023) Δ24FiberRGD (p=0.03) in ovarian cancer cells (Figure 4B). The ability of  $\Delta$ 24DoubleRGD to kill ovarian cancer cells in vitro appeared to be unaffected by double modification of pIX and Fiber. On the other hand, cell killing activity of Δ24IXRGD was attenuated, suggesting that abnormal incorporation of the degradation

product of pIX-RGD on the Δ24IXRGD viral particles observed in Figure 2B may affect its life-cycle in infected cells. Taken together, these data demonstrated that Δ24DoubleRGD retains cell killing activity despite genetic modifications and its cell killing ability is increased over the cell killing ability of  $\Delta 24IXRGD$ and Δ24FiberRGD.

## Δ24DoubleRGD shows oncolytic ability in vivo

The indirect monitoring of death of cancer cells infected with CRAds in an in vivo study is important because it enables progressive ante mortem readouts throughout the duration of an experiment. In this regard, we have chosen to use luciferase-expressing ovarian cancer cells, SKOV3.Luc, in our animal model. Monitoring of luciferase stably-expressing cancer cells has been shown to facilitate detection of tumor establishment in vivo (Contag et al. 2000). Indeed, the luciferase activity in tumor, as detected by bioluminescence imaging, anatomically overlaps with tumor location in vivo (Edinger et al. 1999). Before our in vivo study, we first confirmed whether luciferase activity in SKOV3.Luc cells infected with CRAds declines as CPE of these cells increases. After 10 days postinfection, the remaining luciferase activity in SKOV3.Luc cells infected with Δ24DoubleRGD showed dramatic decrease as compared to that in non-

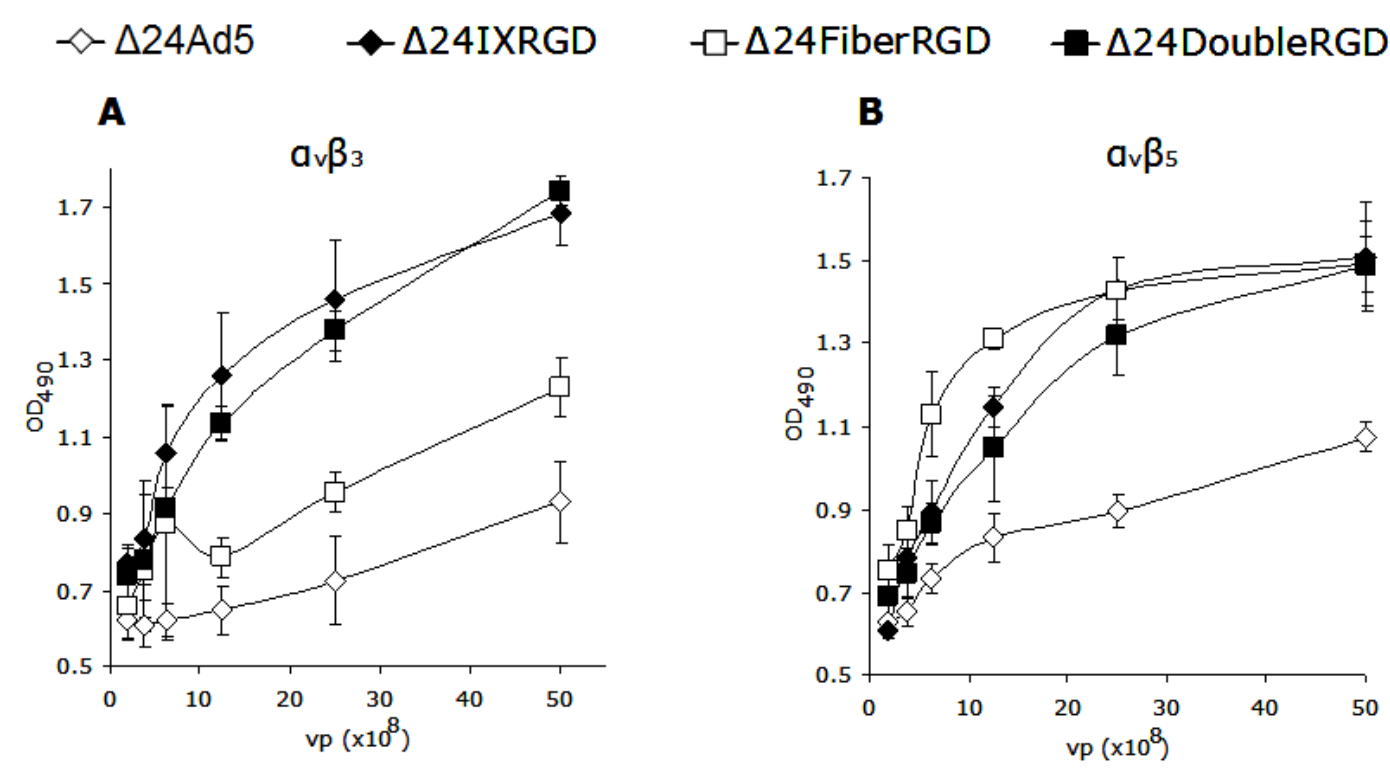


Figure 3. ELISA analysis was used to validate the binding integrity of the CRAds used in this study. Integrins were bound to a 96-well plate followed by binding of CRAds at the listed dilutions. Anti-Ad antibody followed by goat anti-mouse antibody conjugated to Horse Radish Peroxidase allowed for quantitative measurement of the amount of virus bound to integrins using a light-emitting reaction detectable by excitation at OD405. Both  $\Delta 24$ DoubleRGD and  $\Delta 24$ IXRGD bind  $\alpha_{v}\beta_{3}$  integrin significantly better than  $\Delta 24$ Ad5 and  $\Delta 24$ FiberRGD (A). Each of the RGD-modified CRAds bind  $\alpha_v \beta_5$  significantly better than  $\Delta 24Ad5$  (B).

replicative Ad-infected cells (Figure 5). Also, the remaining luciferase activity in SKOV3.Luc cells infected with Δ24DoubleRGD was the lowest value among SKOV3.Luc cells infected with CRAds. The Δ24Double RGD showed increased cell killing versus  $\Delta 24$ Ad5 (p = 0.0009),  $\Delta 24$ IXRGD (p=0.04), and Δ24FiberRGD (p=0.019). These data support the previous produced by the data Δ24RGDCRAd has increased oncolytic ability versus other CRAds (Figure 4) and suggests that luciferase activity may be used to indicate the relative amount of living cells remaining following CRAd infection.

Next we assessed the oncolytic potency of Δ24DoubleRGD in an orthotopic in vivo model of ovarian cancer. SKOV3.Luc cells were used to intraperitoneally establish tumors in female nude mice. Mice were imaged 24 hours post-injection of cells (Day -5) to ensure appropriate cell injection (Figure 6A). On day 6 post-injection of cells (Day 0), mice were imaged to ensure viability of cells and similar expression between groups. Following segregation into groups, mice were injected with  $1.0 \times 10^9$  vp of CRAds or PBS weekly on Days 0, 7, and 14. Representative images indicated that mice injected with Δ24DoubleRGD displayed less luciferase expression than mice treated with PBS beginning at day 21 post-injection (Figure 6A). Quantitative expression of light units was determined by capture of light emitted from mice following injection with luciferin. Data in photons/second were collected and averaged per group of mice. Quantitatively, lower levels of bioluminescence in mice treated with Δ24DoubleRGD as well as each of the other CRAds were detected at 21 days post-injection as

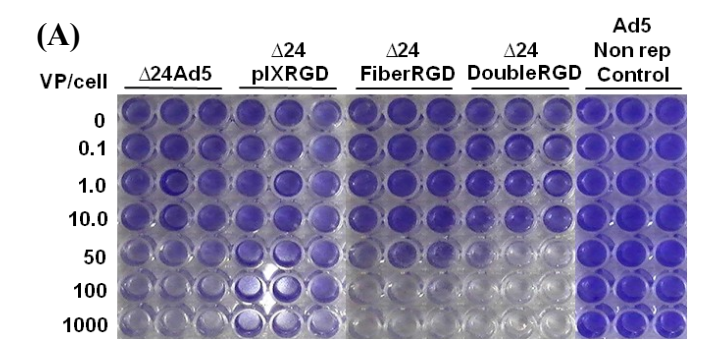
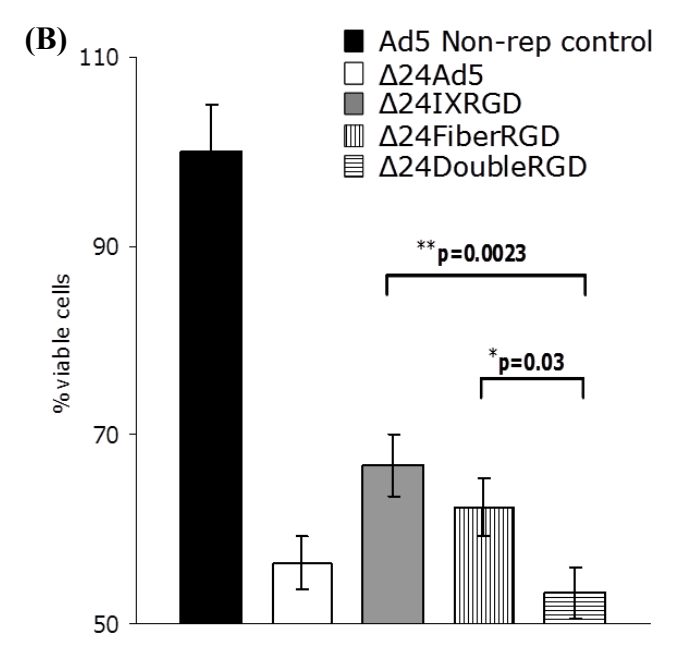


Figure 4. Crystal violet analysis of SKOV3.Luc cells following 10-days of infection with CRAds at listed VP/cell indicated that Δ24DoubleRGD causes more CPE, as determined by less staining of remaining cells, as compared to Ad5 non-replicative control vector, Δ24Ad5, Δ24IXRGD, and  $\Delta 24$ FiberRGD (A).  $\Delta 24$ DoubleRGD also caused increased killing of SKOV3.Luc cells as determined by light emitted from cells following administration of MTS reagent and read on plate reader at OD405 (B). Less light emitted is indicative of increased CPE, less living cells, at the time of reading.

compared to mice treated with PBS (Figure 6B). Mice treated with Δ24DoubleRGD survived longer than the PBS-treated group whose average lifespan was 23 days post-injection of PBS (Figure 6C). Thus, treatment with Δ24DoubleRGD as well as the other CRAds prolonged the survival of mice versus PBS-treated group in this experiment. The overall survival of the mice treated with either of the CRAds averaged 29.5 days.

#### **Discussion**

Novel treatments for ovarian cancer have been used in the past several years in an effort to increase the lifespan of ovarian cancer patients. Targeted therapy is one form of novel treatment that has gained much exposure over the last decade due to its potential to selectively deliver an oncolytic therapy to cancer cells while incurring minimal deleterious effects on non-cancer cells. In this regard, ovarian cancer is an ideal candidate for treatment with targeted therapy as it usually presents with metastases throughout the peritoneum of patients. Ovarian cancer is a good disease model for targeted therapy development because of the expression of a certain class of molecules on the surfaces of ovarian cancer cells in what has been discovered as a cancer-specific pattern. This class of molecules is integrins. Integrins belong to a family of cell surface receptors made up of 18-α and 8-β subunits that mediate attachment of cells to the extracellular matrix or other cells by combining to form at least 24 different heterodimers (Ruoslahti 1996, Hynes 1999). Integrins are expressed on many cell types and under physiological conditions are used to facilitate attachment between



the extracellular matrix or other cells (Ruoslahti 1996, Hynes 1999), as well as to support cell proliferation, migration, and viability (Carmeliet 2000, Friedlander et al. 1995). The  $\alpha_v$  subunit of integrins is overexpressed on ovarian cancer cells (Liapis et al. 1997, Cannistra et al., 1995) and has been identified as a marker for poor prognosis in advanced-stage ovarian carcinoma (Goldberg et al. 2001). Furthermore, Liapis et al. (1997) report increased expression of  $\alpha_v \beta_3$  in ovarian carcinomas as compared to tumors with low malignant potential.  $\alpha_v \beta_3$  has been shown to be expressed in 6 of 9 ovarian cancer specimens and 50% of SKOV3 cells (the parent cell line of the SKOV3.Luc cells used in our study) in a study to determine the expression of integrins in ovarian carcinoma (Cannistra et al. 1995). Several experiments with conflicting results have also been published: β<sub>3</sub> expression is associated with a favorable prognosis in ovarian cancer patients (Kaur et al. 2009) and Carreiras et al. (1996) reported that the  $\beta_3$  integrin is less highly expressed in high-grade versus well-differentiated tumors. These data indicate that variability of integrin expression on ovarian cancer cells is expected. Therefore, despite these conflicting data regarding amounts of receptors on certain types of ovarian carcinomas, we know that some expression of  $\alpha_v \beta_3$  and  $\alpha_v \beta_5$  integrins is evident in our SKOV3.Luc cells because the presence of these integrins is a necessary component of Ad infection (Brüning et al. 2001, Wickham et al. 1993, Takayama et al. 1998).

One clear way to move forward has been to target the integrins found on the cancer cells. The ligand of  $\alpha_v \beta_3$  and  $\alpha_v \beta_5$  integrins was determined to be a tripeptide motif, RGD (Ruoslahti 1996). This RGD

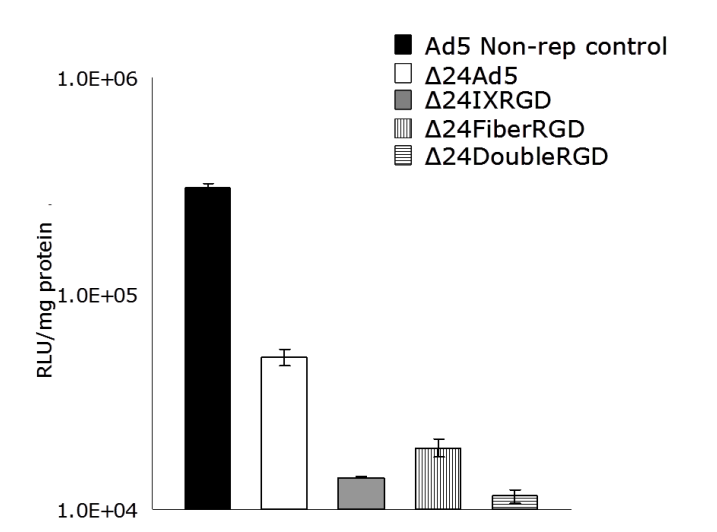


Figure 5. SKOV3.Luc cells, which constitutively express luciferase, were used to determine if luciferase expression is indicative of amount of number of cells remaining alive following 10 days of infection with indicated CRAd.

motif may bind to several integrins (Gamble et al. 2010). The binding ability of RGD to a particular set of integrins is dependent upon several factors, including but not limited to: 1) flanking region of the RGD sequence and 2) accessibility of binding sites. Experiments have shown that different RGD motifs bind differently to the same integrins. In an elaborate experiment to determine which of seven previously reported RGD motifs bound and transduced both CAR positive and CAR negative cells the best, Nagel et al. determined that the RGD4C motif inserted into the HI-loop of fiber, the structure used by Dmitriev et al. (1998) performed better than the other six variations of RGD incorporation (Nagel et al. 2003). The results of their study also indicated that the RGD motif found on penton base, when placed into the HI-loop of fiber, does not bind as well as the RGD4C motif used by Dmitriev et al. Based on these data, we decided to use the RGD4C motif for our experiments as well.

Ads have been proposed as oncolytic virotherapy agents. The ability of Ads to infect a wide range of cells, ability to replicate in dividing and non-dividing cells, and ability to incorporate a large amount of material (i.e. therapeutic genes, imaging modalities) into their genomes underscored their potential utility as oncolytic agents. Discovery that the Ad primary receptor, CAR, is decreased on the surfaces of several cancer cell types (Hemmi et al. 1998, Miller et al. 1998), including ovarian cancer cells (Kim et al. 2002), led to efforts to circumvent this problem. Scientists responded by altering Ad tropism with a tripeptide motif, Arginine-Glycine-Aspartate (RGD). Ad5lucRGD was created and found to have enhanced transduction of ovarian cancer cells and primary tumor tissues (Dmitriev et al. 1998). It was also noted that this virus is capable of successfully transducing ovarian cancer cells in vitro and patient ovarian cancer samples ex vivo in a CAR-independent manner (Dmitriev et al. 1998). The ability to effectively transduce ovarian cancer cells by addition of the RGD4C motif was promising but left another concern, safety.

Replication selectivity is one way to enhance the safety of Ads that are to be used as therapeutic agents. To this end, scientists have made several attempts to render Ads conditionally replicative by deleting the E1A gene, modifying the E1A gene, or inserting tumor specific promoters to regulate the E1A gene. The E1A proteins are necessary for viral replication and are the first to be produced following viral transduction (Dyson & Harlow 1992, Flint & Shenk 1997). In normal viral replication, E1A protein binds to Rb, causing the release of Rb from its dimerization with E2F. This uncoupling leads to cellular transition from the G1/S checkpoint (Nevins 1992). Deletion of 24

bases of the E1A gene resulting in loss of Rb binding site of E1A prevents cellular transition to S phase which results in the inability of virus to replicate in cells with a normal p16/Rb pathway (Fueyo et al. 2000). Many cancer types, including ovarian cancer, do not have a normal p16/Rb pathway. In fact, two studies have shown that nearly 50% of ovarian carcinomas have a dysfunctional p16/Rb (Yaginuma et al. 1997, Niederacher et al. 1999, Corney et al. 2008). This defect in the p16/Rb pathway in ovarian cancer cells that is not present in normal cells allows for cancer cell-selective replication of  $\Delta 24Ad5$ 

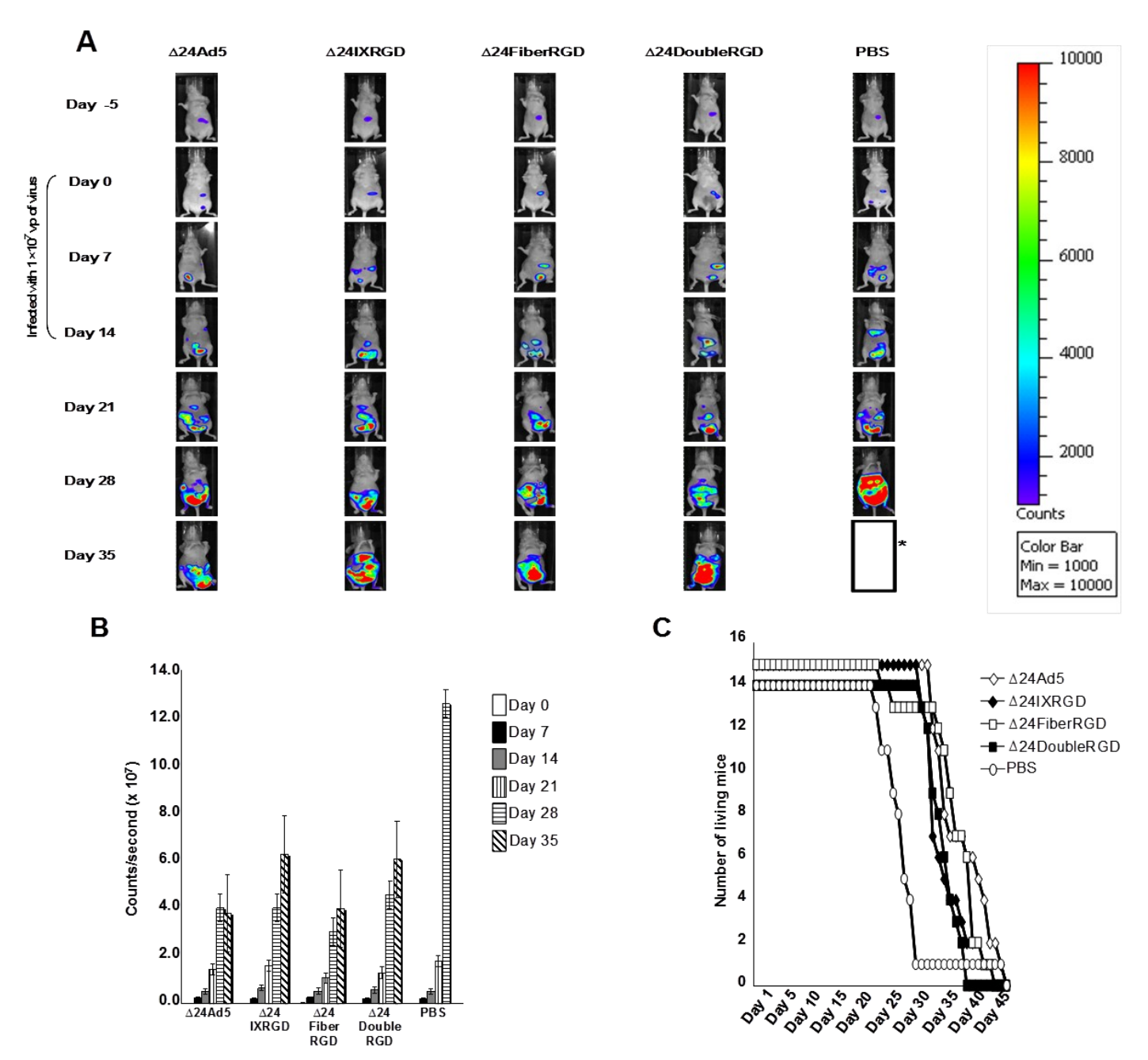


Figure 6. SKOV3.Luc cells (1.0 x 10<sup>7</sup> vp) were injected IP into the abdomen of female BALB/c nude mice. Mice were divided into groups (n=15) and each group was treated with CRAds (1.0 x 10<sup>9</sup> vp) or PBS on Days 0, 7, and 14. Abdominal tumors increased in size in mice from Day 0 to Day 35 as determined by detection of photons following IP injection of luciferase substrate (A). Asterisk (\*) indicates that all mice from PBS group had died by day 35 (with the exception of one outlier). Quantitative analysis of photons emitted by abdominal tumors indicated an increased rate of growth of PBS-injected mice as compared with CRAd-injected mice (B). Asterisk (\*) indicates that all mice from PBS group were dead by day 35 so data could not be generated for this group. Mice injected with  $\Delta 24Ad5$  (p=0.0015),  $\Delta 24IXRGD$  (p=0.032), or  $\Delta 24FiberRGD$  (p=0.007) showed a significant increase in survival as compared to PBS-treated mice. Δ24DoubleRGD showed a non-significant (p=0.11) increase in survival versus PBS-treated mice. Survival of mice treated with each of the CRAds was similar (C).

CRAds (Fueyo et al. 2000). Δ24FiberRGD has been determined to be safe in cotton rats in a study designed to determine toxicity prior to use in clinical trials (Page 2007). Both the safety and utility of Δ24FiberRGD were tested in a clinical trial to treat patients with advanced ovarian cancer (Kimball et al. 2010).

Based on the above information, we endeavored to engineer a virus,  $\Delta 24$ DoubleRGD, that selectively replicates in cancer cells and also targets  $\alpha_{\nu}\beta_{3}$ and  $\alpha_v \beta_5$  integrins, present on ovarian cancer cells, better than the previously tested Δ24FiberRGD as evidenced by increased oncolytic ability. To this end, we successfully incorporated an RGD fusion protein into the pIX region of Δ24FiberRGD (Figure 1). We also created or amplified the other CRAds that were to be controls:  $\Delta 24$ ,  $\Delta 24IXRGD$ , used as Δ24FiberRGD. Coomassie staining indicated that there were similar amounts of structural proteins present in each of the CRAds (Figure 2A). This suggests that incorporation of an RGD motif at Fiber and fusion protein at pIX does not interfere with incorporation of major viral proteins into the Ad capsid. Western blot analysis for pIX indicates that the CRAds differentially incorporate pIX into their capsids based upon integration of the fusion protein (Figure 2B and C). Further validation of CRAd integrity indicated that Flag is present on pIX from Δ24IXRGD and Δ24DoubleRGD (Figure 2C to D), the only CRAds that incorporate these motifs (Figure 1). This finding by both Western blot and ELISA analyses validates incorporation of the fusion protein, containing RGD at the pIX locale, Δ24IXRGD and Δ24FiberRGD. The degradation products seen on the Western blot in the Δ24IXRGD sample and to a lesser degree in the Δ24DoubleRGD sample indicate that some amount of the modified protein may not have formed or folded properly.

Our data indicate differential binding of Δ24FiberRGD to ανβ3 and ανβ5 (Figure 3A to B) and that Δ24FiberRGD selectively binds to ανβ5 integrin, suggesting that the binding characteristics of the RGD motif in the HI-loop may be different from that of the RGD motif fused in pIX of Δ24IXRGD, which binds both ανβ3 and ανβ5 integrins. Moreover, we observed the interaction between the RGD motif of penton base and  $\alpha_v \beta_3$  and  $\alpha_v \beta_5$  integrins at a high concentration, supporting previous data that Ads utilize  $\alpha_v \beta_3$  and  $\alpha_v \beta_5$ as secondary receptors (Nagel et al. 2003, Mathias et al. 1994, Goldman & Wilson 1995). Taken together, these data lead to the conclusion that modification of pIX using the RGD motif expands Ad5 tropism, and Δ24DoubleRGD and Δ24IXRGD are capable of binding not only  $\alpha_{\nu}\beta_{5}$  but also  $\alpha_{\nu}\beta_{3}$  integrins.

comparing Cell viability assays our Δ24DoubleRGD with Δ24FiberRGD suggest enhanced oncolysis of ovarian cancer cells infected with Δ24DoubleRGD in vitro (Figure 4A and B). This conclusion was corroborated by the decrease in luciferase activity of SKOV3.Luc cells following infection and CPE induction (Figure 5). We suspect that the enhanced oncolysis of SKOV3.Luc cells may be due to the ability of  $\Delta 24$ DoubleRGD to bind to both the  $\alpha_{\nu}\beta_{3}$ and  $\alpha_v \beta_5$  integrins while  $\Delta$ FiberRGD shows enhanced binding to  $\alpha_{\nu}\beta_{5}$  preferentially. Similar cell killing ability of all CRAds tested in the orthotopic model of ovarian cancer in nude mice may be due to several factors (Figure 6A to C). While this model replicates the intraperitoneal setting of disease that is seen in ovarian cancer patients, the pre-existing Ad immunity which results in decreased oncolytic ability of  $\Delta 24$  (Elkas et al. 1999) is not seen. Approximately 35% of patients in the US and Europe have pre-existing Ad immunity (Initiative IAV 2010). This fact gives  $\Delta 24$ FiberRGD its clinical advantage over  $\Delta 24Ad5$ , despite their similar cell killing abilities, because previously reported data indicate that the RGD motifs on Fiber protect the CRAd from the antibodies in the ascites found in the peritoneum of ovarian cancer patients (Elkas et al. 1999, Blackwell et al. 2000, Stewart et al. 1997). Because we used a nude mouse model and were not able to pre-expose our mice to Ad5, we were unable to discern the differences between oncolytic ability of Δ2Ad5 versus Δ24FiberRGD nor differences between  $\Delta$ 24DoubleRGD and  $\Delta$ 24FiberRGD in this setting.

This vector is also a unique representation of the Ad5's ability to target cells through a simultaneous expression of the RGD motif on different structural components of the Ad capsid. Generation of this virus and verification of its ability to enhance cell killing versus a singly-modified virus is a proof of principle for the idea that modification of both pIX and Fiber may be used in conjunction to enhance the oncolvtic efficacy of CRAds. Previous reports have indicated that modification of pIX with various motifs can result in enhanced CAR-deficient cell infectivity (Dmitriev et al. 2002), detection (Le et al. 2004), delivery of therapeutics (Li et al. 2005), shielding (Li et al. 2005, Hedley et al. 2006), and even allow mosaic combinations of these modifications by heterologous incorporation into pIX (Kimball et al. 2009, Tang et al. 2008, 2009, Matthews et al. 2006).

In conclusion, our data shows enhanced oncoof Δ24DoubleRGD relative to ability Δ24FiberRGD *in vitro* but similar antitumor potency to that of  $\Delta 24$ FiberRGD in an orthotopic model of ovarian cancer in nude mice. As the virotherapy field continues to advance, animal models that more closely resemble the pathophysiology of human patients must progress towards models that will allow scientists to discern between therapeutics that will or will not work and therapeutics that are or are not safe.

## Acknowledgements

The authors would like to acknowledge the assistance of Karri Folks and other support staff at the UAB Small Animal Imaging shared facility (P30CA013148). The authors reserve special thanks for the following individuals whose input was influential in the experimental design and/or production of the viruses used in these experiments: Angel Rivera, David T. Curiel. The authors are also grateful for the assistance of the Center for AIDS Research (CFAR) and Comprehensive Cancer Center (CCC) DNA Sequencing and Analysis Core at the University of Alabama at Birmingham. The funders had no role in study design, data collection and analysis, decision to publish, or preparation of the manuscript. Grant support was provided by the National Institutes of Health: 5R01CA121187-03S2 5R01CA121187-03, 3P30CA013148-38S9.

#### References

Barnes MN, Coolidge CJ, Hemminki A, Alvarez RD & Curiel DT 2002 Conditionally replicative adenoviruses for ovarian cancer therapy. *Mol Cancer Ther* **1** 435-439.

Bauerschmitz GJ, Lam JT, Kanerva A, Suzuki K, Nettelbeck DM, Dmitriev I, Krasnykh V, Mikheeva GV, Barnes MN, Alvarez RD, et al. 2002 Treatment of ovarian cancer with a tropism modified oncolytic adenovirus. Cancer Res **62** 1266-1270.

Blackwell JL, Li H, Gomez-Navarro J, Dmitriev I, Krasnykh V, Richter CA, Shaw DR, Alvarez RD, Curiel DT & Strong TV 2000 Using a tropism-modified adenoviral vector to circumvent inhibitory factors in ascites fluid. Hum Gene Ther 11 1657-1669.

Borovjagin AV, McNally LR, Wang M, Curiel DT, Mac-Dougall MJ & Zinn KR 2010 Noninvasive monitoring of mRFP1- and mCherry-labeled oncolytic adenoviruses in an orthotopic breast cancer model by spectral imaging. Mol Imaging 9 59-75.

Brüning A, Köhler T, Quist S, Wang-Gohrke S, Moebus VJ, Kreienberg R & Runnebaum IB 2001 Adenoviral transduction efficiency of ovarian cancer cells can be limited by loss of integrin beta3 subunit expression and increased by reconstitution of integrin alphavbeta3. Hum Gene Ther 12 391-399.

Campos SK, Parrott MB & Barry MA 2004 Avidin-based targeting and purification of a protein IX-modified, metabolically biotinylated adenoviral vector. Mol Ther 9 942-954. Cannistra SA, Ottensmeier C, Niloff J, Orta B & DiCarlo J 1995 Expression and function of beta 1 and alpha v beta 3 integrins in ovarian cancer. Gynecol Oncol 58 216-225.

Carmeliet P 2000 Mechanisms of angiogenesis and arteriogenesis. Nat Med 6 389-395.

Carreiras F, Denoux Y, Staedel C, Lehmann M, Sichel F & Gauduchon P 1996 Expression and localization of alpha v integrins and their ligand vitronectin in normal ovarian epithelium and in ovarian carcinoma. Gynecol Oncol 62 260-

Chartier C, Degryse E, Gantzer M, Dieterle A, Pavirani A & Mehtali M 1996 Efficient generation of recombinant adenovirus vectors by homologous recombination in Escherichia coli. J Virol 70 4805-4810.

Choi M, Fuller CD, Thomas CR & Wang SJ 2008 Conditional survival in ovarian cancer: results from the SEER dataset 1988-2001. Gynecol Oncol 109 203-209.

Contag CH, Jenkins D, Contag PR & Negrin RS 2000 Use of reporter genes for optical measurements of neoplastic disease in vivo. Neoplasia 2 41-52.

Corney DC, Flesken-Nikitin A, Choi J & Nikitin AY 2008 Role of p53 and Rb in ovarian cancer. Adv Exp Med Biol **622** 99-9117.

Dmitriev I, Krasnykh V, Miller CR, Wang M, Kashentseva E, Mikheeva G, Belousova N & Curiel DT 1998 An adenovirus vector with genetically modified fibers demonstrates expanded tropism via utilization of a coxsackievirus and adenovirus receptor-independent cell entry mechanism. J Virol 72 9706-9713.

Dmitriev IP, Kashentseva EA & Curiel DT 2002 Engineering of adenovirus vectors containing heterologous peptide sequences in the C terminus of capsid protein IX. J Virol 76 6893-6899.

Dyson N & Harlow E 1992 Adenovirus E1A targets key regulators of cell proliferation. Cancer Surv 12 161-195.

Edinger M, Sweeney TJ, Tucker AA, Olomu AB, Negrin RS & Contag CH 1999 Noninvasive assessment of tumor cell proliferation in animal models. Neoplasia 1 303-310.

Elkas J, Baldwin R, Pegram M, Tseng Y & Karlan B 1999 Immunoglobulin in ovarian cancer ascites inhibits viral infection: implications for adenoviral mediated gene therapy. Gynecol Oncol 72 456.

Flint J & Shenk T 1997 Viral transactivating proteins. Annu Rev Genet 31 177-212.

Friedlander M, Brooks PC, Shaffer RW, Kincaid CM, Varner JA & Cheresh DA 1995 Definition of two angiogenic pathways by distinct alpha v integrins. Science 270 1500-1502.

Fueyo J, Gomez-Manzano C, Alemany R, Lee PS, McDonnell TJ, Mitlianga P, Shi YX, Levin VA, Yung WK & Kyritsis AP 2000 A mutant oncolytic adenovirus targeting the Rb pathway produces anti-glioma effect in vivo. Oncogene 19 2 -12.

Fueyo J, Gomez-Manzano C, Bruner JM, Saito Y, Zhang B, Zhang W, Levin VA, Yung WK & Kyritsis AP 1996 Hypermethylation of the CpG island of p16/CDKN2 correlates with gene inactivation in gliomas. Oncogene 13 1615-1619. Gamble LJ, Borovjagin AB & Matthews QL 2010 Role of RGD-containing ligands in targeting cellular integrins: Applications for ovarian cancer virotherapy (Review). Exp Ther Med 1 233-240.

Goldberg I, Davidson B, Reich R, Gotlieb WH, Ben-Baruch

G, Bryne M, Berner A, Nesland JM & Kopolovic J 2001 Alphav integrin expression is a novel marker of poor prognosis in advanced-stage ovarian carcinoma. Clin Cancer Res 7 4073-4079.

Goldman MJ & Wilson JM 1995 Expression of alpha v beta 5 integrin is necessary for efficient adenovirus-mediated gene transfer in the human airway. J Virol 69 5951-5958.

Hedley SJ, Chen J, Mountz JD, Li J, Curiel DT, Korokhov N & Kovesdi I 2006 Targeted and shielded adenovectors for cancer therapy. Cancer Immunol Immunother 55 1412-1419. Heise C, Hermiston T, Johnson L, Brooks G, Sampson-Johannes A, Williams A, Hawkins L & Kirn D 2000 An adenovirus E1A mutant that demonstrates potent and selective systemic anti-tumoral efficacy. Nat Med 6 1134-1139.

Heise C & Kirn DH 2000 Replication-selective adenoviruses as oncolytic agents. J Clin Invest 105 847-851.

Hemmi S, Geertsen R, Mezzacasa A, Peter I & Dummer R 1998 The presence of human coxsackievirus and adenovirus receptor is associated with efficient adenovirus-mediated transgene expression in human melanoma cell cultures. Hum Gene Ther 9 2363-2373.

Hynes RO 1999 Cell adhesion: old and new questions. Trends Cell Biol 9 33-37.

Initiative IAV 2010 Understanding Pre-existing Immunity. AIDS Vaccine Clinical Trials.

Jemal A, Siegel R, Ward E, Hao Y, Xu J, Murray T & Thun MJ 2008 Cancer statistics, 2008. CA Cancer J Clin 58 71-

Kaur S, Kenny HA, Jagadeeswaran S, Zillhardt MR, Montag AG, Kistner E, Yamada SD, Mitra AK & Lengyel E 2009 {beta}3-integrin expression on tumor cells inhibits tumor progression, reduces metastasis, and is associated with a favorable prognosis in patients with ovarian cancer. Am J Pathol 175 2184-2196.

Kelly FJ, Miller CR, Buchsbaum DJ, Gomez-Navarro J, Barnes MN, Alvarez RD & Curiel DT 2000 Selectivity of TAG-72-targeted adenovirus gene transfer to primary ovarian carcinoma cells versus autologous mesothelial cells in vitro. Clin Cancer Res 6 4323-4333.

Khuu H, Conner M, Vanderkwaak T, Shultz J, Gomez-Navarro J, Alvarez RD, Curiel DT & Siegal GP 1999 Detection of Coxsackie-Adenovirus Receptor (CAR) Immunoreactivity in Ovarian Tumors of Epithelial Derivation. Appl Immun Mol Morph 7 266.

Kim M, Zinn KR, Barnett BG, Sumerel LA, Krasnykh V, Curiel DT & Douglas JT 2002 The therapeutic efficacy of adenoviral vectors for cancer gene therapy is limited by a low level of primary adenovirus receptors on tumour cells. Eur J Cancer 38 1917-1926.

Kimball KJ, Preuss MA, Barnes MN, Wang M, Siegal GP, Wan W, Kuo H, Saddekni S, Stockard CR, Grizzle WE, Harris RD, Aurigemma R, Curiel DT & Alvarez RD 2010 A phase I study of a tropism-modified conditionally replicative adenovirus for recurrent malignant gynecologic diseases. Clin Cancer Res 16 5277-5287.

Kimball KJ, Rivera AA, Zinn KR, Icyuz M, Saini V, Li J, Zhu ZB, Siegal GP, Douglas JT, Curiel DT, et al. 2009 Novel infectivity-enhanced oncolytic adenovirus with a capsid-incorporated dual-imaging moiety for monitoring virotherapy in ovarian cancer. Mol Imaging 8 264-277.

Kirn D 2000 Replication-selective oncolytic adenoviruses: virotherapy aimed at genetic targets in cancer. Oncogene 19 6660-6669.

Le LP, Everts M, Dmitriev IP, Davydova JG, Yamamoto M & Curiel DT 2004 Fluorescently labeled adenovirus with pIX-EGFP for vector detection. *Mol Imaging* **3** 105-116.

Li J, Le L, Sibley DA, Mathis JM & Curiel DT 2005 Genetic incorporation of HSV-1 thymidine kinase into the adenovirus protein IX for functional display on the virion. Virology 338 247-258.

Liapis H, Adler LM, Wick MR & Rader JS 1997 Expression of alpha(v)beta3 integrin is less frequent in ovarian epithelial tumors of low malignant potential in contrast to ovarian carcinomas. Hum Pathol 28 443-449.

Liu Y, Heyman M, Wang Y, Falkmer U, Hising C, Szekely L & Einhorn S 1994 Molecular analysis of the retinoblastoma gene in primary ovarian cancer cells. Int J Cancer 58 663-667.

Maizel JJ, White D & Scharff M 1968 The polypeptides of adenovirus. I. Evidence for multiple protein components in the virion and a comparison of types 2, 7A, and 12. Virology **36** 115-125.

Mathias P, Wickham T, Moore M & Nemerow G 1994 Multiple adenovirus serotypes use alpha v integrins for infection. J Virol 68 6811-6814.

Matthews QL, Sibley DA, Wu H, Li J, Stoff-Khalili MA, Waehler R, Mathis JM & Curiel DT 2006 Genetic incorporation of a herpes simplex virus type 1 thymidine kinase and firefly luciferase fusion into the adenovirus protein IX for functional display on the virion. Mol Imaging 5 510-519.

Meulenbroek RA, Sargent KL, Lunde J, Jasmin BJ & Parks RJ 2004 Use of adenovirus protein IX (pIX) to display large polypeptides on the virion--generation of fluorescent virus through the incorporation of pIX-GFP. Mol Ther 9 617-624. Miller CR, Buchsbaum DJ, Reynolds PN, Douglas JT, Gillespie GY, Mayo MS, Raben D & Curiel DT 1998 Differential susceptibility of primary and established human glioma cells to adenovirus infection: targeting via the epidermal growth factor receptor achieves fiber receptor-independent gene transfer. Cancer Res 58 5738-5748.

Nagel H, Maag S, Tassis A, Nestle FO, Greber UF & Hemmi S 2003 The alphavbeta5 integrin of hematopoietic and nonhematopoietic cells is a transduction receptor of RGD-4C fiber-modified adenoviruses. Gene Ther 10 1643-

NCI 2009 Ovarian Cancer Homepage. Cancer Topics. Bethesda Maryland.

Nevins JR 1992 E2F: a link between the Rb tumor suppressor protein and viral oncoproteins. Science 258 424-429.

Niederacher D, Yan HY, An HX, Bender HG & Beckmann MW 1999 CDKN2A gene inactivation in epithelial sporadic ovarian cancer. Br J Cancer 80 1920-1926.

Page JG, Tian B, Schweikart K, Tomaszewski J, Harris R, Broadt T, Polley-Nelson J, Noker PE, Wang M, Makhija S, Aurigemma R, Curiel DT & Alvarez RD 2007 Identifying the safety profile of a novel infectivity-enhanced conditionally replicative adenovirus, Ad5-delta24-RGD, in anticipation of a phase I trial for recurrent ovarian cancer. Am J Obstet Gynecol 196 389.e1-9; discussion 389.e9-10.

Ruoslahti E 1996 RGD and other recognition sequences for integrins. Annu Rev Cell Dev Biol 12 697-715.

Sherr CJ 1996 Cancer cell cycles. Science 274 1672-1677.

Stewart PL, Chiu CY, Huang S, Muir T, Zhao Y, Chait B, Mathias P & Nemerow GR 1997 Cryo-EM visualization of an exposed RGD epitope on adenovirus that escapes antibody neutralization. EMBO J 16 1189-1198.

Suzuki K, Fueyo J, Krasnykh V, Reynolds PN, Curiel DT & Alemany R 2001 A conditionally replicative adenovirus with enhanced infectivity shows improved oncolytic potency. Clin Cancer Res 7 120-126.

Takayama K, Ueno H, Pei XH, Nakanishi Y, Yatsunami J & Hara N 1998 The levels of integrin alpha v beta 5 may predict the susceptibility to adenovirus-mediated gene transfer in human lung cancer cells. Gene Ther 5 361-368.

Tang Y, Le LP, Matthews QL, Han T, Wu H & Curiel DT 2008 Derivation of a triple mosaic adenovirus based on modification of the minor capsid protein IX. Virology 377 391-400.

Tang Y, Wu H, Ugai H, Matthews QL & Curiel DT 2009 Derivation of a triple mosaic adenovirus for cancer gene therapy. PLoS One 4.

Ulasov IV, Rivera AA, Han Y, Curiel DT, Zhu ZB & Lesniak MS 2007 Targeting adenovirus to CD80 and CD86 receptors increases gene transfer efficiency to malignant glioma cells. J Neurosurg 107 617-627.

Vanderkwaak TJ, Wang M, Gomez-Navarro J, Rancourt C, Dmitriev I, Krasnykh V, Barnes M, Siegal GP, Alvarez R & Curiel DT 1999 An advanced generation of adenoviral vectors selectively enhances gene transfer for ovarian cancer gene therapy approaches. Gynecol Oncol 74 227-234.

Vellinga J, Rabelink MJWE, Cramer SJ, van den Wollenberg DJM, Van der Meulen H, Leppard KN, Fallaux FJ & Hoeben RC 2004 Spacers increase the accessibility of peptide ligands linked to the carboxyl terminus of adenovirus minor capsid protein IX. J Virol 78 3470-3479.

Wang M, Hemminki A, Siegal GP, Barnes MN, Dmitriev I, Krasnykh V, Liu B, Curiel DT & Alvarez RD 2005 Adenoviruses with an RGD-4C modification of the fiber knob elicit a neutralizing antibody response but continue to allow enhanced gene delivery. Gynecol Oncol 96 341-348.

Whyte P, Buchkovich KJ, Horowitz JM, Friend SH, Raybuck M, Weinberg RA & Harlow E 1988 Association between an oncogene and an anti-oncogene: the adenovirus E1A proteins bind to the retinoblastoma gene product. Nature 334 124-129.

Whyte P, Williamson NM & Harlow E 1989 Cellular targets for transformation by the adenovirus E1A proteins. Cell 56

Wickham TJ, Mathias P, Cheresh DA & Nemerow GR 1993 Integrins alpha v beta 3 and alpha v beta 5 promote adenovirus internalization but not virus attachment. Cell 73 309-319.

Yaginuma Y, Hayashi H, Kawai K, Kurakane T, Saitoh Y, Kitamura S, Sengoku K & Ishikawa M 1997 Analysis of the Rb gene and cyclin-dependent kinase 4 inhibitor genes (p16INK4 and p15INK4B) in human ovarian carcinoma cell lines. Exp Cell Res 233 233-239.